

Study of self-similar and self-affine objects using logarithmic correlation integral

Victor Sapozhnikov and Efi Foufoula-Georgiou

St. Anthony Falls Hydraulic Laboratory, University of Minnesota, Minneapolis, MN 55414, USA

Received 22 April 1994, in final form 27 October 1994

Abstract. We suggest a logarithmic correlation integral $z(x, y)$ as a good tool for investigating self-affine and self-similar objects. First, it enables us to extract fractal exponents ν_x and ν_y from one pattern of an object having any topology. Second, we show that the integral $z(x, y)$ which completely characterizes a monofractal object provides more information on the density correlation properties of the object than just the exponents ν_x and ν_y . We quantify this additional information by introducing two parameters: δ , characterizing the object's anisotropy of a non-scaling nature, and κ characterizing the curvature of the logarithmic correlation integral of the object. We demonstrate that the four parameters: ν_x , ν_y , δ and κ provide an effective parametrization of the logarithmic correlation integral of a self-affine monofractal object. We give some examples of self-affine objects, having the same fractal exponents ν_x and ν_y but different parameters δ and κ indicating the differences in the correlation properties of the objects. We demonstrate that even a self-similar object showing isotropic scaling ($\nu_x = \nu_y$) may have the non-scaling anisotropy parameter δ different from zero, which indicates that the object has an asymmetric integral $z(x, y)$ and, therefore, different correlation properties in different directions. It is shown that the equality $\kappa = 0$ outlines a class of objects for which the exponents ν_x and ν_y are not defined uniquely. For instance, such objects can be treated as both self-similar and self-affine. If κ is close to zero, estimation of the exponents ν_x and ν_y may become problematic. Relationships connecting the exponents ν_x , ν_y and fractal dimensions of the projection and cross section of an object are established.

1. Introduction

Many objects, such as relief vertical cross sections, rivers and river networks, growing surfaces and interfaces, dendritic structures, trails of Brownian motion and others are self-affine fractals [1]. Each part of a self-affine object is an image of the whole object (either strictly or in a statistical sense) scaled differently in different directions. In other words, if we take a part of the object within an $X \times Y$ rectangle and then change X and Y in a certain different way, we will get the same pattern. This finds its mathematical expression in the relationship

$$M(X, Y) \sim X^{1/\nu_x} \sim Y^{1/\nu_y} \quad (1)$$

where $M(X, Y)$ is the mass of the part of the object within the $X \times Y$ rectangle, and ν_x , ν_y are the fractal exponents.

While there are several methods for determination of the fractal dimension of self-similar objects, methods for determination of the fractal exponents characterizing self-affine objects seem to be much less developed. The fractal dimension of a self-similar object can be easily found using one pattern. However, in a general case, e.g. for branched structures,

one cannot find the fractal exponents ν_x and ν_y from one pattern of a self-affine object. The problem is that the mass M only scales if the sides of the rectangle change in a certain different way and, in contrast to the self-similar case, we do not know *a priori* how to change X and Y because we do not know the ratio ν_x/ν_y . We can only state that the mass within the rectangle scales *provided* $X^{1/\nu_x} \sim Y^{1/\nu_y}$. Therefore, it seems that if one faces the problem of determination of the fractal exponents of a natural or simulated self-affine object using one pattern one would usually fail to do that. An appropriate method has only been developed for a special case when the self-affine object represents a non-branched line (e.g. see [2]).

The methods available for studying a general self-affine object do not analyse the geometry of the object, but rather follow how the mass M_0 of the total object changes as the sizes X_0 and Y_0 of the object change. If one has available either an ensemble of the same type of objects of different size, or the patterns of the object at different stages of growth, the ensemble or the evolution of the object can be characterized by exponents α_x and α_y using the relationship

$$M(X_0, Y_0) \sim X_0^{1/\alpha_x} \sim Y_0^{1/\alpha_y}. \quad (2)$$

We will call α_x and α_y *external exponents*, in contrast to the *internal exponents* ν_x and ν_y which characterize the geometry of the object. As shown in section 2 the internal and external scaling exponents have different meanings and are not always equal. A method for extracting the exponents ν_x and ν_y from one pattern of a fractal object is developed in section 3. We also introduce two parameters, δ and κ which complement the information contained in the fractal exponents ν_x and ν_y . We establish relationships connecting the exponents ν_x and ν_y and fractal dimensions of the projection and cross section of an object. In section 4 we demonstrate the applicability of the developed method using some fractal objects for which ν_x and ν_y are known theoretically. We show that the estimated values of ν_x and ν_y correspond to the theoretical ones. We also estimate the parameters δ and κ for these objects. In section 5 we show the significance of the introduced parameters δ and κ . Using these parameters we indicate some types of fractal objects showing rather unexpected correlation properties. Finally, some conclusions are drawn in section 6.

2. Internal fractal exponents versus external exponents

Since methods for extracting the internal exponents from one pattern of the object are not available in the general case, external exponents instead of internal ones are often used to describe the geometry of the object (see, e.g. [3–5]). However, this approach supposes that internal and external exponents are equivalent. We will present theoretical evidence and two examples demonstrating that this supposition is, generally speaking, wrong.

(i) The external exponents may be different from the internal ones. To compare the external exponents α_x and α_y with the internal ones, ν_x and ν_y , let us examine a growing self-similar object as a particular case of a self-affine object. If the size of the object is R and the mass is $M(R)$, then the mass within the square of size r covering a part of the object will be $m(r, R) = M(R)(r/R)^{1/\nu}$. If $M(R) \sim R^{1/\alpha}$, then

$$m(r, R) \sim R^{1/\alpha - 1/\nu}. \quad (3)$$

The last relationship shows that $\alpha = \nu$ if and only if m does not depend on R , which means that the external and the internal exponents are equal when, in the course of its evolution, the object neither grows nor dissolves inside. If this is not the case, the internal and external exponents differ.

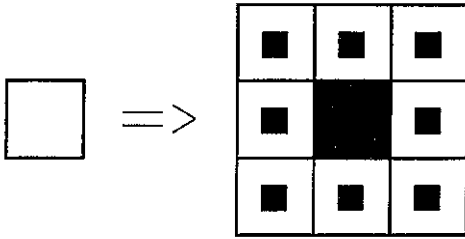


Figure 1. One step of a process where growth of an object in size is accompanied by its internal dissolution. Due to the dissolution the external exponents $\alpha_x = \alpha_y = \log 3 / \log(64/9)$ characterizing the process are different from the internal fractal exponents $\nu_x = \nu_y = \log 3 / \log 8$ describing the geometry of the object.

As an illustration let us build an ensemble of Sierpinsky carpets. Let the first one be just a square. To build the next carpet we take two steps. At the first step we put together 8 squares to build a regular 3×3 Sierpinsky carpet and at the second step we divide the initial squares in 9 squares and delete the middle one (which corresponds to the dissolution of the object in the course of its growth)—see figure 1. Repeating this process will give us an ensemble of Sierpinsky carpets with $\nu_x = \nu_y = \log 3 / \log 8$. However, the mass of each next carpet will be not 8, but $8 \times (8/9)$ times greater than the mass of the previous one, and therefore for this process $\alpha_x = \alpha_y = \log 3 / \log(64/9)$. Clearly, ν_x and ν_y are different from α_x and α_y in this case.

(ii) In some cases the ensemble of objects or the object growth is characterized by the external exponents, and the internal exponents of the objects are not defined uniquely at all. As the simplest case here let us consider compact objects. For example, Scheidegger river networks obtained by computer simulation are shown to be compact objects and their ensemble is characterized by the values $\alpha_x = \frac{2}{3}, \alpha_y = \frac{1}{3}$ [3,4]. It is implied (e.g. see the discussion after (4) in [3]) that these exponents characterize the fractal geometry of the networks. However, the compactness of a two-dimensional object means that the object is just a piece of a plane. This, in turn, means that, in contrast to the external exponents α_x and α_y that characterize the evolution (or the ensemble) of the networks, the internal exponents characterizing their geometry are not defined uniquely. For example, it is quite obvious that a piece of a plane can be treated as a self-similar object as well and be characterized by $\nu_x = \nu_y = 1/D = 1/2$. It will be shown formally in section 5 that any fractal exponents satisfying the relationship $\nu_x + \nu_y = 1$ describe a compact object. The non-uniqueness of the fractal exponents ν_x and ν_y can arise for non-compact objects too. As shown in section 5 there exists a class of non-compact fractal objects for which the internal exponents ν_x and ν_y are still not defined uniquely and derive general conditions under which an object falls into this class (equations (29) and (30)). The internal exponents of such objects are bounded only by relation (31).

The above theoretical evidence and examples demonstrate clearly that the external exponents α_x and α_y not only require a set of patterns for their estimation, but, generally speaking, are something different from the internal exponents ν_x and ν_y . Therefore elaboration of a method that would enable us to extract the internal fractal exponents from one pattern of an object is highly desirable. Such a method is developed in the next section.

3. Correlation characteristics of self-affine objects

3.1. A method for estimating the fractal exponents ν_x and ν_y

Let us write the scaling equation describing a self-affine object in the form

$$\left(\frac{X_2}{X_1}\right)^{1/\nu_x} = \left(\frac{Y_2}{Y_1}\right)^{1/\nu_y} = \frac{M_2}{M_1} \tag{4}$$

Introducing $x = \log X$, $y = \log Y$ and $z = \log M$, we get

$$\frac{x_2 - x_1}{\nu_x} = \frac{y_2 - y_1}{\nu_y} = z_2 - z_1 \quad (5)$$

or

$$\frac{dx}{\nu_x} = \frac{dy}{\nu_y} = dz. \quad (6)$$

The function $M(X, Y)$ is known as the correlation integral [6]. Here by analogy we call the function $z(x, y)$ the logarithmic correlation integral of the object under study.

Equations (5) and (6) describe a cylindric surface $z(x, y)$, i.e. a surface that has constant derivative in a specific direction (the direction of the cylinder generating line). The second equality in (6) is true only if the first one is true. Comparing (6) with the equation

$$\frac{\partial z}{\partial x} dx + \frac{\partial z}{\partial y} dy = dz \quad (7)$$

valid for any values of dx and dy , we obtain

$$\nu_x \frac{\partial z}{\partial x} + \nu_y \frac{\partial z}{\partial y} = 1. \quad (8)$$

The last relationship provides a method for estimating the fractal exponents ν_x and ν_y of a self-affine object. Indeed, having estimated the logarithmic correlation integral $z(x, y)$ from a pattern of the object (by direct calculation of the mass $M(X, Y)$ within rectangles of sizes $X \times Y$), one can calculate the derivatives $\partial z(x, y)/\partial x$ and $\partial z(x, y)/\partial y$ and use them to find the values of ν_x and ν_y . Ideally, two points (x, y) giving different values of the derivatives $\partial z(x, y)/\partial x$ and $\partial z(x, y)/\partial y$ are sufficient, but for a good estimation it is preferable to compute the derivatives at all (x, y) points and follow a least-squares estimation technique. Such a technique is employed in section 4 to extract the fractal exponents from a pattern of some simulated fractal objects.

3.2. Quantifying the other correlation characteristics of self-affine objects

The solution of (8), as well as of (6), is

$$z(x, y) = \frac{x}{2\nu_x} + \frac{y}{2\nu_y} + \omega \left(\frac{x}{2\nu_x} - \frac{y}{2\nu_y} \right) \quad (9)$$

or

$$M(X, Y) = X^{1/2\nu_x} Y^{1/2\nu_y} \Omega \left(X^{1/2\nu_x} Y^{-1/2\nu_y} \right) \quad (10)$$

where $\omega(\xi)$ and $\Omega(\xi) \equiv \exp(\omega(\log \xi))$ are arbitrary functions.

Relationship (9) shows that the fractal exponents ν_x and ν_y contain only a part of the information on the correlation properties of a fractal object. The rest of the information is contained in the function $\omega(\xi)$. Indeed, in section 5 we give an example of fractal objects having the same values of ν_x and ν_y and different correlation properties because their $\omega(\xi)$ functions are different. It can be seen from (6) and (9) that while the fractal exponents ν_x and ν_y determine the direction of the generating line of the cylindric surface $z(x, y)$, the function $\omega(\xi)$ provides the additional information needed to describe the shape of any cross section of the cylindric surface. Thus, together ν_x , ν_y and $\omega(\xi)$ completely determine the shape of the logarithmic correlation integral $z(x, y)$.

Let us study some general features of the behaviour of the function $\omega(\xi)$ and $z(x, y)$. The nature of the function $M(X, Y)$ imposes some restrictions on $\omega(\xi)$. Indeed, by its

meaning, the function $M(X, Y)$ cannot have negative derivatives. As it follows from (9), the requirements $\partial M(X, Y)/\partial X > 0$ and $\partial M(X, Y)/\partial Y > 0$ lead to the inequality $-1 < \omega(\xi) < 1$. Assuming, that $\omega(\xi)$ does not oscillate at infinity, we find, that it has two asymptotes, $\omega'(+\infty)$ and $\omega'(-\infty)$. This gives us an important feature of $\omega(\xi)$ and of the $z(x, y)$ surface, namely, that $\omega(\xi)$ saturates to two lines at positive and negative infinities, i.e. $z(x, y)$ is composed of two planes (one when $\xi = x/2\nu_x - y/2\nu_y$ is a large positive value and the other when it is a large negative value) and an intermediate zone between them.

Since the $z(x, y)$ surface is a cylinder it can be described using only two coordinates (ξ, η) in the appropriate coordinate system (ξ, ζ, η) . We obtain this coordinate system from the original (x, y, z) by (i) rotating the (x, y, z) system about the z -axis until the y -axis coincides with the projection of the generating line on the x - y plane, and (ii) rotating the system about the new x -axis until the y -axis coincides with the generating line. It can be shown that in this new coordinate system the equation for the logarithmic correlation integral takes the form

$$\eta(\xi) = \frac{\nu_y^2 - \nu_x^2}{2\nu_x\nu_y\sqrt{1 + \nu_x^2 + \nu_y^2}} \xi + \frac{\sqrt{\nu_y^2 + \nu_x^2}}{\sqrt{1 + \nu_x^2 + \nu_y^2}} \omega\left(\frac{\sqrt{\nu_y^2 + \nu_x^2}}{2\nu_x\nu_y} \xi\right). \quad (11)$$

As we see, because the ζ -axis coincides with the cylinder generating line, the equation for the cylinder surface is expressed in terms of ξ and η only. The function $\eta(\xi)$ is exactly what one sees when one views the $z(x, y)$ surface from the direction of the generating line. Since the ξ - η plane is orthogonal to the direction of the generating line, it is preferable to use $\eta(\xi)$ instead of $\omega(\xi)$ to describe the correlation properties of an object, since these properties are now not only complementary to the scaling exponents ν_x and ν_y (determining the direction of the generating line of the cylinder), but also independent of them.

Since the $z(x, y)$ surface has two asymptotic planes, its cross section $\eta(\xi)$ saturates to two asymptotic lines. Therefore $\eta'(\xi)$ has two asymptotic values, $\eta'(+\infty)$ and $\eta'(-\infty)$.

To quantify the correlation characteristics of a self-affine object, other than the fractal exponents ν_x and ν_y we introduce two parameters

$$\begin{aligned} \delta &= \frac{\eta'(-\infty) + \eta'(+\infty)}{2} \\ &= \frac{\nu_y^2 - \nu_x^2}{2\nu_x\nu_y\sqrt{1 + \nu_x^2 + \nu_y^2}} + \frac{\nu_y^2 + \nu_x^2}{2\nu_x\nu_y\sqrt{1 + \nu_x^2 + \nu_y^2}} \frac{\omega'(-\infty) + \omega'(+\infty)}{2} \end{aligned} \quad (12)$$

and

$$\kappa = \frac{\eta'(-\infty) - \eta'(+\infty)}{2} = \frac{\nu_y^2 + \nu_x^2}{2\nu_x\nu_y\sqrt{1 + \nu_x^2 + \nu_y^2}} \frac{\omega'(-\infty) - \omega'(+\infty)}{2}. \quad (13)$$

The value of δ characterizes the anisotropy of the cross section of the function $z(x, y)$ ($\delta = 0$ when the cross section is isotropic), and κ is a measure of curvature of the $z(x, y)$ function ($\kappa = 0$ when the surface is flat). These two parameters are important characteristics of a self-affine object. They complement the information contained in the fractal exponents ν_x and ν_y . The parameter δ describes a different type of anisotropy of a self-affine object than the ratio of the scaling exponents ν_x/ν_y . In fact, in section 5 we show that even a self-similar object ($\nu_x = \nu_y$) may have anisotropic correlation characteristics which is indicated by $\delta \neq 0$. To distinguish between these two types of anisotropy we coined the terms *scaling anisotropy parameter* for ν_x/ν_y and *non-scaling anisotropy parameter* for δ . Regarding the curvature parameter κ , in section 5 we show that if it is equal to zero, i.e.

the cylindric surface $z(x, y)$ degenerates into a plane, the exponents ν_x and ν_y of the fractal object are not defined uniquely.

3.3. Further study of the shape of the surface $z(x, y)$. Connection between the exponents ν_x and ν_y and other characteristics of fractal objects

Let us now find the equations for the plane parts of the surface $z(x, y)$. To do that we consider the slope of each plane in the x and y directions. By definition of the function $M(X, Y)$ the derivatives $\partial z(x, 0)/\partial x$ and $\partial z(0, y)/\partial y$ are fractal dimensions of cross sections of the object in the directions of X and Y axes, D_{cx} and D_{cy} , respectively. As shown in the appendix the derivatives $\partial z(0, y)/\partial x$ and $\partial z(x, 0)/\partial y$ are correlation fractal dimensions D_2 [6] of the projections of the object on X and Y axes, D_{px2} and D_{py2} , respectively. Putting $z(0, 0) = 0$ (which is just a matter of normalization of $M(X, Y)$) we get the equations for the two asymptotic planes

$$z_-(x, y) = D_{px2}x + D_{cy}y \tag{14}$$

$$z_+(x, y) = D_{cx}x + D_{py2}y. \tag{15}$$

Let us remind the reader that the generalized fractal dimensions D_q are

$$D_q = \lim_{\epsilon \rightarrow 0} \frac{\log(\sum p_i^q)}{(q - 1) \log \epsilon} \quad q \neq 1 \tag{16}$$

$$D_1 = \lim_{\epsilon \rightarrow 0} \frac{\sum p_i \log p_i}{\log \epsilon}. \tag{17}$$

Here p_i is the fraction of the measure in a box of size ϵ (in our case it is the fraction of the object that projects into an interval of size ϵ). D_0 is the fractal dimension of the support of the measure, D_1 and D_2 are called information and correlation dimensions, respectively.

The relationships (14) and (15) enable us to demonstrate clearly what one gets when one determines the fractal dimension of a self-affine object: one finds how the mass within an $X \times Y$ rectangle changes as its sides change *proportionally to each other*. In other words, one just finds the slope of the section of the plane $z(x, y)$ by the plane $y = x + a$, where constant $a = \log(Y/X)$. If $\nu_x > \nu_y$ then for positive values of a ($Y > X$) the plane $y = x + a$ will only intersect the $z_-(x, y)$ plane, while for negative values of a both $z_-(x, y)$ and $z_+(x, y)$ planes will be intersected. This creates two slopes, corresponding to what is called global and local fractal dimensions of a self-affine object D_G and D_L , correspondingly [8]. Putting $y = x + a$ in (14) and (15), we obtain that for $\nu_x > \nu_y$

$$D_G = D_{px2} + D_{cy} \tag{18}$$

$$D_L = D_{py2} + D_{cx}. \tag{19}$$

It follows from (14), (15) and (8) that for the case $D_{px2} = D_{py2} = 1$ this result coincides with the expressions $D_G = (\nu_y - \nu_x + 1)/\nu_y$, $D_L = (\nu_x - \nu_y + 1)/\nu_x$ from [8].

Having substituted (9) in (14) and (15), and differentiated the equations with respect to x and y one can see that the fractal dimensions of the cross sections and of the projections, D_{cx} , D_{cy} and D_{px2} , D_{py2} are connected with the $\omega(\xi)$ function by the following relationships:

$$\omega'(-\infty) = -2\nu_y D_{cy} + 1 = 2\nu_x D_{px2} - 1 \tag{20}$$

$$\omega'(+\infty) = 2\nu_x D_{cx} - 1 = -2\nu_y D_{py2} + 1 \tag{21}$$

so knowing, say, ν_x , ν_y , D_{px2} and D_{py2} one can easily calculate the parameters δ and κ from (12), (13) and (20), (21).

Substituting (14) and (15) into (8) we obtain the important relationships

$$\nu_x D_{cx} + \nu_y D_{py2} = 1 \quad (22)$$

$$\nu_x D_{px2} + \nu_y D_{cy} = 1 \quad (23)$$

which can be used for estimation of ν_x and ν_y given D_{cx} , D_{cy} , D_{px2} and D_{py2} . For a self-similar object (22) and (23) give

$$D_{cx} + D_{py2} = D_{cy} + D_{px2} = D \quad (24)$$

where D is the fractal dimension of the object. We note that the last equation is different from the equation obtained by Mandelbrot [8]: $D_{cx} + D_{py1} = D$ where D_{py1} is the information dimension [6] of the projection on the Y -axis. In the next section we consider some examples confirming our result (22)–(24).

4. Analysis of correlation properties of some fractal objects

To illustrate the application of the proposed approach for analysing self-affine objects we study the correlation properties of three fractal objects whose fractal exponents we know in advance. The objects are shown in the upper row of figure 2: (a) simulated river ($\nu_x = \nu_y = 0.77$), (b) trace of Brownian motion ($\nu_x = 1$, $\nu_y = \frac{1}{2}$) and (c) 3×5 Sierpinsky carpet ($\nu_x = \log 5 / \log 6 = 0.898$, $\nu_y = \log 3 / \log 6 = 0.613$). (The simulated river channel shown in figure 2(a) is built by a special type of a self-avoiding walk. If a walking particle crossed its own trajectory, the formed loop was erased. The final trajectory of a random walk was regarded as a river. See [2, 9] for details).

Taking advantage of (8) we find the values of the exponents ν_x and ν_y for the objects shown in figure 2(a) and (b)—see figure 3. They are (a) $\nu_x = \nu_y = 0.77$ and (b) $\nu_x = 1.00$, $\nu_y = 0.48$, in agreement with the theoretical values.

Let us first visualize the surfaces $z(x, y)$ of the objects (see figures 2(a)–(c), bottom row). Since the functions $z(x, y)$ of fractal objects are cylindric surfaces we can view them in the direction of the cylinder generating line (see (5) and (6)). In other words, it is possible to adjust the rotation angle φ about the z -axis and the tilt angle ψ above the x - y plane from which the surface is viewed to see only the edge of the surface (which is the $\eta(\xi)$ function). It is not difficult to show that the following relationships connecting the angles and the exponents hold:

$$\tan \varphi = \nu_x / \nu_y \quad (25)$$

$$\sin \psi = (1 + \nu_x^2 + \nu_y^2)^{-1/2} \quad (26)$$

or, reversely

$$\nu_x = \sin \varphi \cot \psi \quad (27)$$

$$\nu_y = \cos \varphi \cot \psi \quad (28)$$

The second row of figure 2(a)–(c) shows the surfaces viewed from the angles φ and ψ determined by (25) and (26). It can be seen that $z(x, y)$ really represent cylindric surfaces and that the angles φ and ψ correspond to the relationships (25)–(28).

The surface $z(x, y)$ of the Sierpinsky carpets is step-like because of the step-like procedure of their construction. This produces a large spread in the values of the derivatives $\partial z / \partial x$ and $\partial z / \partial y$ and does not allow us to find its fractal exponents from (8). However, looking at its $z(x, y)$ surface in figure 2(c), middle row, one can see that apart from its

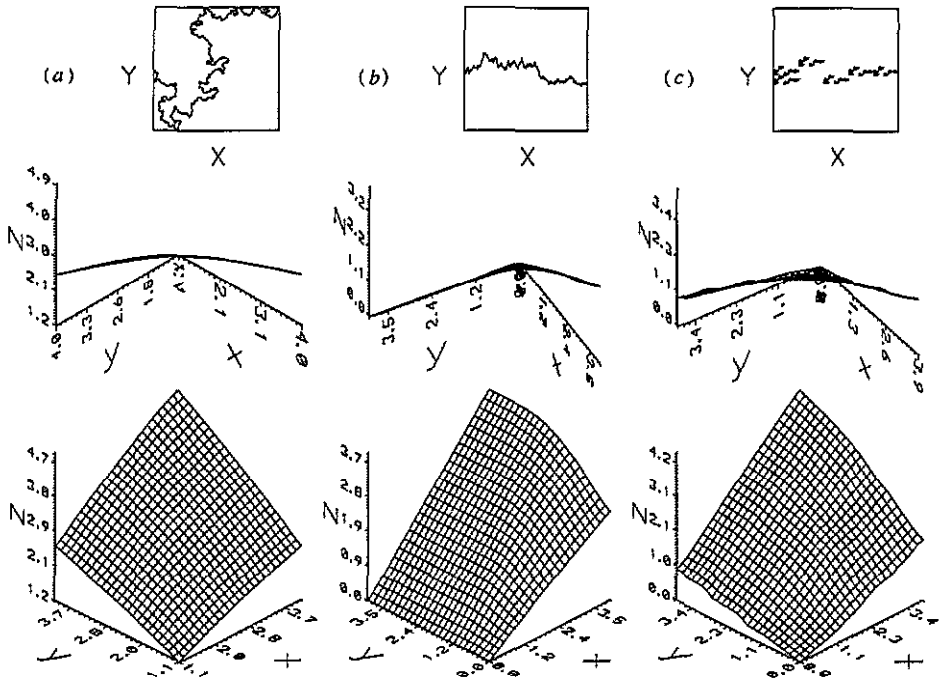


Figure 2. Fractal objects and their $z(x, y)$ functions: (a) simulated river ($\nu_x = \nu_y = 0.77$, $\delta = 0$, $\kappa = 0.27$), (b) Brownian motion trace ($\nu_x = 1$, $\nu_y = 1/2$, $\delta = -0.083$, $\kappa = 0.417$) and (c) 3×5 Sierpinsky carpet ($\nu_x = \log 5 / \log 6 = 0.898$, $\nu_y = \log 3 / \log 6 = 0.613$, $\delta = -0.038$, $\kappa = 0.266$). The second row shows the surfaces viewed from the angles φ and ψ determined by (25) and (26).

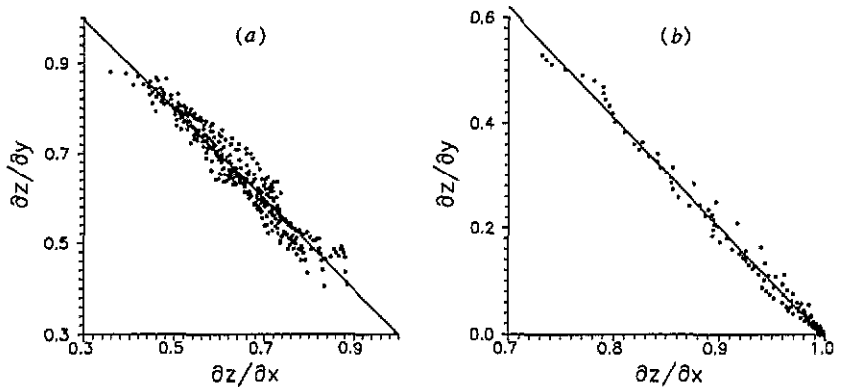


Figure 3. Estimation of the fractal exponents ν_x and ν_y for (a) simulated river—see figure 2(a), and (b) trace of Brownian motion—see figure 2(b). Advantage is taken of (8). The estimated values are (a) $\nu_x = \nu_y = 0.77$ and (b) $\nu_x = 0.48$, $\nu_y = 1.00$.

step-like form it is a cylindrical surface, with the direction of generating line corresponding to (25)–(28).

As can be seen from (14) and (15) the slopes of the intersection of the $z(x, y)$ surface with the XZ and YZ planes are D_{cx} and D_{cy} , respectively. Having found these values for

Table 1. Summary of correlation characteristics ν_x , ν_y , δ and κ , of the fractal objects simulated in the paper.

Object	Figure	ν_x	ν_y	ν_y/ν_x	δ	κ
River channel	2(a)	0.77	0.77	1	0	0.27
Trace of Brownian motion	2(b)	1	0.5	0.5	-0.083	0.417
5×3 Sierpinsky carpet	2(c)	0.898	0.613	0.683	-0.038	0.266
3×3 Sierpinsky carpet	4(a)	1	1	1	0	0.577
3×3 Sierpinsky carpet	4(b)	1	1	1	-0.268	0.310
3×3 Sierpinsky carpet	4(c)	1	1	1	0	0.040

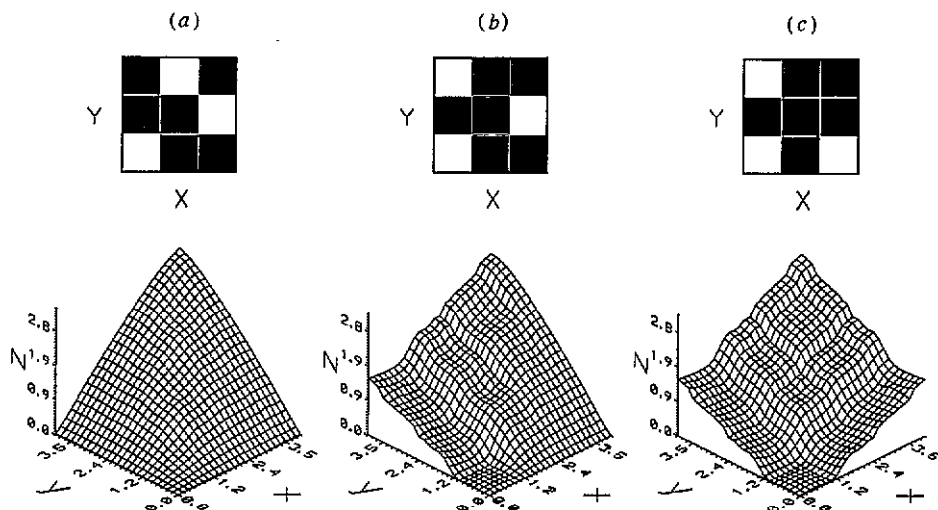


Figure 4. Logarithmic correlation integrals $z(x, y)$ of different self-similar Sierpinsky carpets having fractal dimension $D = 1$ (bottom figures) and the corresponding generators (top figures). The deleted parts are marked black. Though the carpets have the same fractal dimension their correlation properties are different, which is reflected in the difference of their $z(x, y)$ functions. The asymmetric function $z(x, y)$ for the carpet (b) shows that this self-similar fractal is anisotropic.

the three analysed objects we used (20) and (21) to estimate $\omega'(+\infty)$ and $\omega'(-\infty)$ and then (12) and (13) to determine the parameters δ and κ characterizing the anisotropy and the curvature of their logarithmic correlation integrals $z(x, y)$. The values of the parameters are: for the river $\delta = 0$, $\kappa = 0.27$, for the trace of Brownian motion $\delta = -0.083$, $\kappa = 0.417$, and for the Sierpinsky carpet $\delta = -0.038$, $\kappa = 0.266$ (see table 1 for a summary). For all three objects the curvature parameter is significantly different from zero. As will be seen in the next section this is a necessary condition for being able to estimate the fractal exponents ν_x and ν_y . The anisotropy parameter δ is equal to zero for the self-similar object, the river channel. One could think that a self-similar object is bound to have symmetric correlation properties and therefore its non-scaling anisotropy parameter δ should always be equal to 0. However, as shown in the next section this is not true.

We make use of the above fractal objects to demonstrate that relationships (22)–(24) hold. For instance, from the $z(x, y)$ function of the river channel (figure 2(a)) we found $D_{px2} = D_{py2} = 0.91$ and $D_{cx} = D_{cy} = 0.39$, which are in a good agreement with the fractal exponents of the channel $\nu_x = \nu_y = 0.77$ found above. We also projected the picture of

the river and found the values D_{px2} and D_{py2} directly by calculating the sum from the right part of (A4). The direct calculation gives $D_{px2} = D_{py2} = 0.92$, in good agreement with the values found from the analysis of the function $z(x, y)$.

Application of the same procedure to some Sierpinsky carpets confirms the results (22)–(24), as well. In these cases we were also able to make sure that the determined values of the derivatives $\partial z(0, y)/\partial x$ agree with the theoretical values of the correlation dimension D_{px2} , and not with the informative dimension D_{px1} as implied by Mandelbrot in [8]. For instance, for the Sierpinsky carpet, shown in figure 4(c) $\partial z(0, y)/\partial x = 0.53$; the projection of the carpet and the direct calculation gives the same value. The theoretical value $D_{px2} = D_{py2} = -\log(\sum p_i^2)/\log 3 = 0.535$, while the informative dimension $D_{px1} = D_{py1} = -(\sum p_i \log p_i)/\log 3 = 0.579$. The dimensions of the cross sections found from the analysis of the $z(x, y)$ function are $D_{cx} = D_{cy} = 0.47$, so $D_{cx} + D_{py2} = 1$, in agreement with (24).

5. Surprising correlation properties of some fractal objects

5.1. A class of fractal objects for which the scaling exponents ν_x and ν_y are not defined uniquely

As pointed out in section 3, having found the values of D_{cx} , D_{cy} , D_{px2} and D_{py2} one can calculate the fractal exponents ν_x and ν_y from (22) and (23). However, this system of linear equations has an infinite set of solutions if the fractal dimensions of the cross sections are equal to the fractal dimensions of the corresponding projections

$$D_{cx} = D_{px2} \equiv D_x \quad (29)$$

$$D_{cy} = D_{py2} \equiv D_y \quad (30)$$

If equations (29) and (30) hold the cylindrical surface $z(x, y)$ degenerates into a plane. Indeed, comparing (13), (20) and (21) with (8) one can easily see that the conditions (29) and (30) are equivalent to one condition: the curvature parameter $\kappa = 0$, which means that the function $\omega(\xi)$ is a straight line, i.e. $z(x, y)$ is a plane. In this case, equations (22) and (23) are reduced to one equation

$$\nu_x D_x + \nu_y D_y = 1 \quad (31)$$

having an infinite set of solutions ν_x and ν_y . Equations (29) and (30) (or, equivalently, the condition $\kappa = 0$) specify a class of fractal objects for which it is impossible to point out a unique pair of fractal exponents. These objects can be described by any exponents which are in agreement with (31). In other words, when the surface $z(x, y)$ degenerates into a plane, the difference between the self-affine and self-similar object disappears and there is no preferable direction for cutting the surface because the trace is a straight line in any direction. For instance, a compact object is characterized by $D_{cx} = D_{cy} = D_{px2} = D_{py2} = 1$. Comparing this relationship with (31), we obtain $\nu_x + \nu_y = 1$. This means that a compact object can be treated as a self-affine one with arbitrary ratio ν_x/ν_y , including e.g. $\nu_x/\nu_y = 1$ (self-similar case). The only significant relationship for such an object is that the sum of the exponents ν_x and ν_y is 1.

It is important to emphasize that relationships (29) and (30) can also be true for a non-compact object. For example, the Sierpinsky carpet having a 3×5 generator with four non-empty cells in the corners (see figure 5) has $D_{cx} = D_{px2} = \log 2/\log 5$, $D_{cy} = D_{py2} = \log 2/\log 3$, and the only thing one can say about the fractal exponents ν_x and ν_y is that they must satisfy (31).

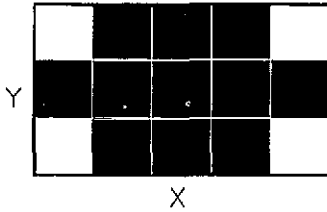


Figure 5. For this Sierpinsky carpet (29) and (30) hold, i.e. fractal dimensions of cross sections are equal to the corresponding fractal dimensions of projections ($D_{cx} = D_{px2} = \log 2 / \log 5$, $D_{cy} = D_{py2} = \log 2 / \log 3$) and, equivalently, the curvature parameter $\kappa = 0$. Therefore its logarithmic correlation integral $z(x, y)$ degenerates into a plane and there is no unique pair of the exponents ν_x and ν_y for this object. Any pair of the exponents bound by relationship (31): $(\log 2 / \log 5)\nu_x + (\log 2 / \log 3)\nu_y = 1$ characterizes this object.

As we have seen, the curvature parameter κ is an important characteristic of correlation properties of an object. Indeed, if $\kappa = 0$, the fractal object can be characterized by an infinite number of exponents ν_x and ν_y . Moreover, even if $\kappa \neq 0$, but is close enough to zero, that is, the $z(x, y)$ function is flat, the estimation of the fractal exponents may become impossible (though in this case they exist). For example, if one uses (8) to estimate the exponents ν_x and ν_y one may find that since the surface $z(x, y)$ is not curved enough, the variations in the true values of the partial derivatives $\partial z(x, y) / \partial x$ and $\partial z(x, y) / \partial y$ over the surface $z(x, y)$ are small and therefore masked by statistical fluctuations.

5.2. Fractal objects having the same scaling exponents ν_x and ν_y and different correlation properties. Anisotropic self-similar objects

We have shown that in some cases one surface $z(x, y)$ can be characterized by different fractal exponents ν_x and ν_y . We will now demonstrate that different surfaces may correspond to the same exponents. Indeed, Sierpinsky carpets whose generators and corresponding $z(x, y)$ surfaces are shown in figures 4(a)–(c) have the same fractal exponents $\nu_x = \nu_y = 1/D = 1$. Calculating D_{p2} as $-\log(\sum p_i^2) / \log 3$, where $p_i = n_i/n$ (n_i is the number of non-empty squares in the i th row and n is the total number of non-empty squares in a generator), and using (12), (13), (20) and (21), we find: (i) $D_{px2} = D_{py2} = 1$, $\delta = 0$, $\kappa = 0.577$, (ii) $D_{px2} = 0.535$, $D_{py2} = 1$, $\delta = -0.268$, $\kappa = 0.310$, and (iii) $D_{px2} = D_{py2} = 0.535$, $\delta = 0$, $\kappa = 0.040$. So, objects having the same fractal dimension may have different parameters κ and δ and, hence, different surface $z(x, y)$. Moreover, the example shown in figure 4(b) demonstrates that density correlation characteristics even of a self-similar object can be different in different directions. This anisotropy is reflected in the asymmetry of the function $z(x, y)$ and is characterized by the value of the non-scaling anisotropy parameter $\delta = -0.268$.

6. Conclusion

The approach proposed, based on the study of the logarithmic correlation integral (i) provides a method for extracting the fractal exponents ν_x and ν_y characterizing the geometry of a self-affine or self-similar object from one pattern only and (ii) permits a better understanding of the correlation properties of such objects. To the best of our knowledge no such method is available in the literature and this may have resulted in the erroneous use of the external exponents α_x and α_y (which can be estimated from an ensemble or evolving pattern) for the description of the geometry of a self-affine object. As demonstrated in this paper the external and internal exponents are generally not equal, except in the special case that the object evolves in a way that it neither grows nor dissolves inside. Even in such a case the suggested approach enables one to find the external exponents (unless (29) and (30) hold) and thus, to predict the evolution of the object from one pattern only instead of an ensemble

of patterns.

Apart from the ability to estimate ν_x and ν_y the use of the logarithmic correlation integral provides more information about the correlation structure of an object than simply ν_x and ν_y . This additional information was quantified by introducing two parameters, one of them (δ) measuring the anisotropy of the object of non-scaling nature and the other (κ) measuring the curvature of the logarithmic correlation integral. Several examples were presented to illustrate the fact that even self-similar fractals for which $\nu_x = \nu_y$ (i) may have different correlation properties and (ii) may still exhibit anisotropy in their correlation structure. The four parameters ν_x , ν_y , δ and κ were connected to fractal dimensions of projections and cross sections of the object. Conditions under which a fractal object has non-unique ν_x and ν_y parameters were derived.

In this paper our analysis focused on the characterization of a monofractal object. The same analysis could be applied to a multifractal object to characterize the behaviour of the first moments only of its correlation structure. However, to fully characterize a multifractal self-affine object one could introduce a function $z(x, y; q)$ where the parameter q characterizes the order of the moment. Following the same approach as here a reduced efficient parametrization of a self-affine multifractal object could be obtained in terms of four functions: $\nu_x(q)$, $\nu_y(q)$, $\delta(q)$ and $\kappa(q)$. This extension is currently under investigation.

Acknowledgments

We would like to thank A Carsteanu and V Nikora for helpful discussions. This research was partially supported by NSF grants BSC-8957469 and EAR-9117866 and NASA grant NAG-52108.

Appendix.

The density correlation function of the object $c(X, Y) = \partial^2 M(X, Y) / \partial X \partial Y$ is the probability to find a particle at the point $(X_0 + X, Y_0 + Y)$ provided there is a particle at the point (X_0, Y_0) . For the lattice model it can be estimated as

$$c(X, Y) = \frac{1}{N} \sum_{X_0, Y_0} \delta(X_0, Y_0) \delta(X_0 + X, Y_0 + Y) \quad (\text{A1})$$

where N is the total number of the particles in the object, $\delta(X_0, Y_0) = 1$ if there is a particle at the point (X_0, Y_0) and $\delta(X_0, Y_0) = 0$ otherwise. Hence $M(X, Y)$ can be estimated as

$$\sum_{U=0}^X \sum_{V=0}^Y c(U, V) = \frac{1}{N} \sum_{U=0}^X \sum_{X_0, Y_0} \delta(X_0, Y_0) \sum_{V=0}^Y \delta(X_0 + U, Y_0 + V). \quad (\text{A2})$$

For large values of Y so that $Y \simeq Y_{0, \max}$, where $Y_{0, \max}$ is the size of the object in the Y -direction

$$\sum_{V=0}^Y \delta(X_0 + U, Y_0 + V) \simeq N_X(X_0 + U) \quad (\text{A3})$$

where $N_X(X_0 + U)$ is the number of particles of the object that project onto the lattice point $X_0 + U$ of X -axis. Therefore, for large values of Y the function $M(X, Y)$ can be estimated as

$$\frac{1}{N} \sum_{U=0}^X \sum_{X_0} \sum_{Y_0} \delta(X_0, Y_0) N_X(X_0 + U) = \frac{1}{N} \sum_{X_0} N_X(X_0) \sum_{U=0}^X N_X(X_0 + U). \quad (\text{A4})$$

The right-hand side of the last equation up to a constant coefficient coincides with the expression for the correlation integral from [7] which in a one-dimensional case is $C(X) = N^{-2} \sum_{i,j=1}^N \theta(X - |X_{0i} - X_{0j}|)$ where $\theta(X)$ is the Heaviside function and X_{0i}, X_{0j} are the coordinates of the particles. The value $C(X)$ is the number of pairs (i, j) whose distance $|X_{0i} - X_{0j}|$ is less than X . When calculating the right-hand side of expression (A4) one performs the same procedure as when he calculates $C(X)$ for the projection of the particles of the object on X -axis. As is shown in [6,7], $C(X)$ scales as X^{D_2} . In other words, $M(X, Y) \sim X^{D_{px2}}$ and $\partial z(x, y)/\partial x = D_{px2}$ for $Y \simeq Y_{0,max}$. Since for $y/v_y \gg x/v_x$ the surface $z(x, y)$ is a plane and the derivative $\partial z(x, y)/\partial x$ is constant the equality $\partial z(x, y)/\partial x = D_{px2}$ is valid not only for $y \simeq \log Y_{0,max}$, but also for any $y \gg (v_y/v_x)x$.

References

- [1] Mandelbrot B B 1977 *Fractals: Form, Chance, and Dimension* (New York: Freeman)
- [2] Nikora V I, Sapozhnikov V B and Noever D A 1993 *Water Resources Res.* **29** 3561
- [3] Kondoh H, Matsushita M and Fukuda Y 1987 *J. Phys. Soc. Japan* **56** 1913
- [4] Meakin P, Feder J and Jossang T 1991 *Physica* **176A** 463
- [5] Nikora V I and Sapozhnikov V B 1992 *Water Resources Res.* **29** 3569
- [6] Grassberger P and Procaccia I 1982 *Physica* **9D** 189
- [7] Grassberger P and Procaccia I 1982 *Phys. Rev. Lett.* **9D** 346
- [8] Mandelbrot B B 1986 Self-affine fractal sets *Fractals in Physics* (Amsterdam: North-Holland) p 3
- [9] Sapozhnikov V B and Nikora V I 1993 *J. Phys. A: Math. Gen.* **26** L623